Development 133, 3371-3377 (2006) doi:10.1242/dev.02514

Milton controls the early acquisition of mitochondria by *Drosophila* oocytes

Rachel T. Cox and Allan C. Spradling*

Mitochondria in many species enter the young oocyte en mass from interconnected germ cells to generate the large aggregate known as the Balbiani body. Organelles and germ plasm components frequently associate with this structure. Balbiani body mitochondria are thought to populate the germ line, ensuring that their genomes will be inherited preferentially. We find that *milton*, a gene whose product was previously shown to associate with Kinesin and to mediate axonal transport of mitochondria, is needed to form a normal Balbiani body. In addition, germ cells mutant for some *milton* or *Kinesin heavy chain* (*Khc*) alleles transport mitochondria to the oocyte prematurely and excessively, without disturbing Balbiani body-associated components. Our observations show that the oocyte acquires the majority of its mitochondria by competitive bidirectional transport along microtubules mediated by the Milton adaptor. These experiments provide a molecular explanation for Balbiani body formation and, surprisingly, show that viable fertile offspring can be obtained from eggs in which the normal program of mitochondrial acquisition has been severely perturbed.

KEY WORDS: Mitochondria, Oogenesis, Fusome, Balbiani body, Microtubule, Kinesin, Dynein

INTRODUCTION

Mitochondria and other cytoplasmic organelles within the newly fertilized egg are provided exclusively by the oocyte. However, very little is known about the mechanisms developing oocytes use to acquire, control and multiply their organelles. A special structure is thought to be involved, the Balbiani body or mitochondrial cloud, that is also associated with other organelles and germ plasm components (reviewed by Guraya, 1979; Kloc et al., 2004). Later, during early embryogenesis, Balbiani body mitochondria enter primordial germ cells, suggesting a role in organellar inheritance. Although long known in *Xenopus* and human oocytes, the existence of a Balbiani body was only recently documented in a model genetic organism, *Drosophila* (Cox and Spradling, 2003).

The backdrop for Balbiani body formation is the germline cyst or nest, a collection of premeiotic germ cells interconnected by intercellular bridges. In *Drosophila*, cysts consisting of 16 germ cells interconnected by ring canals large enough to pass organelles are established by four synchronous rounds of division with incomplete cytokinesis. The germ cells comprising each cyst reorganize their cytoskeletons during each cell cycle, giving rise to the cyst-spanning structure known as the fusome (de Cuevas and Spradling, 1998). The initial daughter of the stem cell, which contains the largest fusome segment, sustains meiosis and differentiates as an oocyte, while the other 15 become nurse cells (de Cuevas and Spradling, 1998; Huynh et al., 2001; Cox and Spradling, 2003).

Within the completed 16-cell cysts, cytoskeletal polarity and motor-dependent directional transport play central roles in determining the oocyte and provisioning it with mitochondria, organelles and specific RNAs (reviewed by Huynh and St Johnston, 2004). Over a 2- to 3-day interval, centrioles leave their juxtanuclear locations and migrate along the fusome toward the oocyte (Mahowald and Strassheim, 1970; Grieder et al., 2000; Bolivar et al., 2001). During the same period, the minus ends of fusome-associated microtubules increasingly focus at the oocyte (Theurkauf et al., 1993; Grieder et al., 2000). Mitochondria and other organelles associate and also move along the fusome (Fig. 1A) (Cox and Spradling, 2003). After accumulating outside the oocyte ring canals, these materials suddenly flow into the oocyte en masse in newly forming follicles, where they join the oocytes pre-existing mitochondria to give rise to the Balbiani body (Fig. 1E). Much later, in stage 7 follicles, the microtubules within the oocyte reorganize again (compare Fig. 1I with 1M), and older oocytes acquire additional mitochondria by replication and transfer from the nurse cells. Acquiring mitochondria in this manner may have been conserved in evolution, because germline cysts, organized microtubule arrays and Balbiani bodies are found at corresponding stages of oocyte development in many species (Guraya, 1979; Matova and Cooley, 2001; Kloc et al., 2004).

Microtubule-based transport has been studied in a wide variety of contexts. Mitochondria are often positioned through the action of protein complexes that link them to microtubule motors (reviewed by Hollenbeck and Saxton, 2005). There is increasing evidence that these complexes interact with motors of opposite polarities, the relative activity of which is regulated (reviewed by Gross, 2004). In *Drosophila* neurons, a specific adaptor protein, Milton, co-localizes with mitochondria, binds Kinesin heavy chain and plays a crucial role in positioning these organelles (Stowers et al., 2002; Gorska-Andrzejak et al., 2003; Glater et al., 2006). In mammals, a family of related proteins known as GRIF proteins link mitochondria to distinct kinesin-containing transport complexes (Brickley et al., 2005). We found that Milton associates with mitochondria in *Drosophila* oocytes (see Fig. S1 in the supplementary material) and, consequently, examined its role in Balbiani body formation.

MATERIALS AND METHODS

Drosophila strains and generation of clones

Fly stocks were cultured at 22-25°C on standard food. To generate negatively marked mutant clones, *shi*; *FRT40A milt*^{92}/*CyO*, *y w*; *FRT40A milt*^{k06704}/*CyO* and *y w*; *FRT40A milt*^{k14514}/*CyO* (Stowers et al., 2002) were

Howard Hughes Medical Institute Research Laboratories, Department of Embryology, Carnegie Institution of Washington, 3520 San Martin Drive, Baltimore, MD 21218, USA

*Author for correspondence (e-mail: spradling@ciwemb.edu)

Accepted 3 July 2006

crossed to *hsFLP*; *FRT40A armlacZ*, and *w*; *FRT42B e Khc^{27}/CyO* was crossed to *hsFLP*; *FRT42B GFP*. The appropriate adult progeny were heat shocked for 1 hour at 37°C three times over 36 hours. After at least 10 days post-heat shock, well-fed females were dissected. To generate *ovo^{D}* clones, *hsFLP; ovo^{D1} FRT40A/CyO* males were crossed to *FRT40A milt/CyO* females. First and second instar progeny were heat shocked once at 37°C for 1 hour. *Khc ovo^{D}* clones were generated according to Serbus et al. (Serbus et al., 2005). *y w*; *milt^{EY01559}* was generated from the *Drosophila* genome project (Bellen et al., 2004). *Oregon R*, *ry$^{506\text{-}CS}$* and *y; ry^{506}* were used as wild-type controls. All other genes and balancer chromosomes are described at FlyBase (http://flybase.bio.indiana.edu/).

Fluorescence microscopy

Females were dissected and fixed as previously described (Cox and Spradling, 2003). Primary antibodies were diluted at follows: mouse anti-Milton 5A124 [1:10; Stowers et al. (Stowers et al., 2002)]; rabbit anti-ATP synthase, β subunit (1:600, gift of Dr Rafael Garesse); mouse 1B1 (1:100, Developmental Studies Hybridoma Bank); rabbit anti-Mannosidase II [1:1000 (Moreman et al., 1991)]; rat anti-Cup [1:1000 (Keyes and Spradling, 1997)]; mouse anti-phosphotyrosine PY20 (1:1000 ICN Biomedicals); mouse anti-β-galactosidase (1:400, Sigma); rabbit anti-Dynein heavy chain (PEP1) [1:500 (McGrail and Hays, 1997)]; mouse anti-Milton 5A124 [1:100 (Stowers et al., 2002)]; and donkey anti-goat GFP (1:2000, Research Diagnostics). The following secondary antibodies were used: goat anti-rabbit, goat anti-mouse and donkey anti-goat AlexaFluor488 (1:400, Molecular Probes); goat anti-rabbit, anti-mouse and anti-rat Cy3 and Cy5; and donkey anti-goat, anti-mouse and anti-rabbit Cy3 and Cy5 (1:1000, Jackson ImmunoResearch). For DNA labeling, DAPI was added 5 μg/ml for 10 minutes. Confocal analysis was carried out using Leica TCS NT and Leica TCS SP2 confocal microscopes. All confocal images are projected *z*-stacks except for Fig. 1J-P, where single optical sections are shown.

Western immunoblotting and RT-PCR

Western blotting was carried out as described (Wilhelm et al., 2000) with the following modifications. To isolate protein, fattened fly ovaries were dissected in Grace's, the Grace's was removed and the ovaries put on dry ice. Boiling Laemmli buffer + BME was added and the ovaries were ground in the Eppendorf tube with a pestle, then put back on dry ice. Sample was boiled for 7 minutes before loading on a 4-15% acrylamide gel. Anti-Milton 5A124 was used 1:200 overnight at 4°C. As a loading control, mouse monoclonal JLA-20 (actin, Sigma) was used 1:200. For RT-PCR, fattened ovaries were dissected in Grace's, then RNA was isolated using Trizol reagent (Invitrogen), by following the included protocol. RT-PCR was performed using the Qiagen OneStep RT-PCR kit. rp49 primers were used simultaneously with the *milton* primers as a control for the amount of RNA in the reaction.

Pole cell counts

milt mutant embryos for *milt^{92}* and *milt^{k06704}* were generated from mothers producing *ovo^{D}* clones. Zero to 3-hour-old embryos were collected and labeled with anti-phosphotyrosine, anti-Vasa (1:250) and DAPI. Pole cells were counted for 10-15 cellularizing embryos of each genotype.

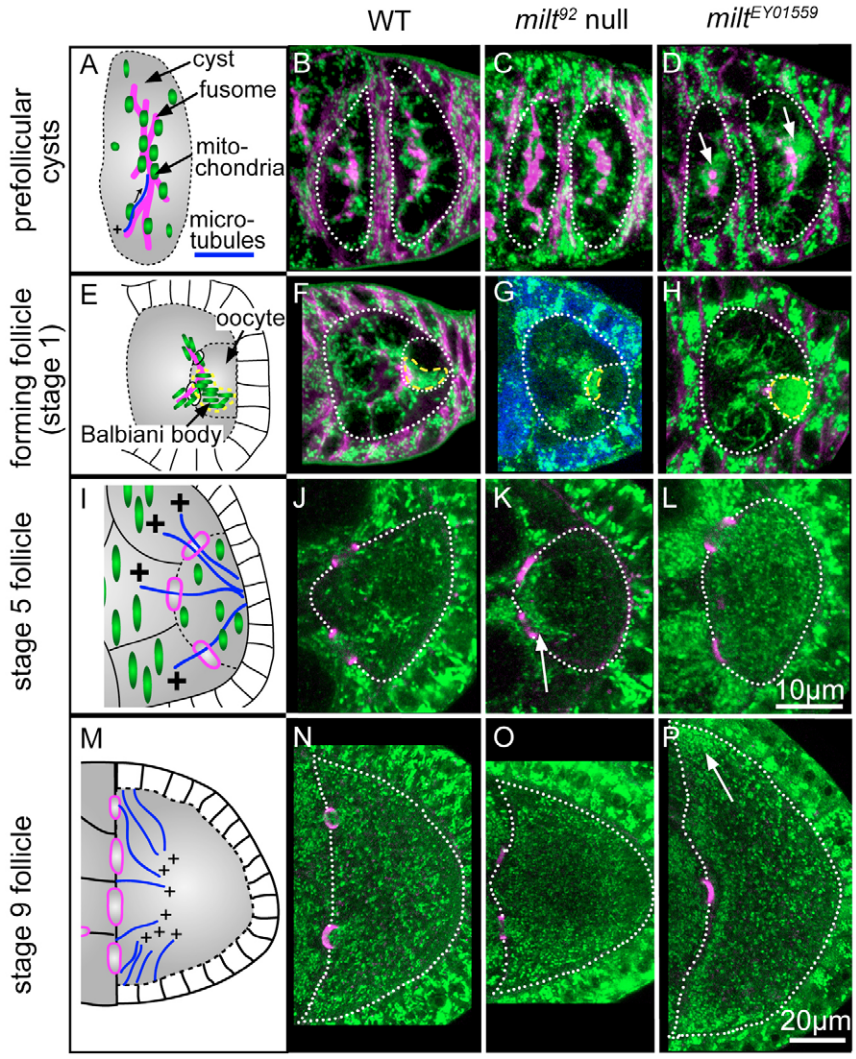

Fig. 1. *milt* mutant oocytes do not form normal Balbiani bodies. (**A-D**) Prefollicular cysts: (A) schematic; mitochondria (green) in wild-type cysts (broken outlines, B) and *milt^{92}* null mutant cysts (broken outlines, C) associate, as expected, with the fusome (magenta). By contrast, mitochondria in class II *milt^{EY01559}* cysts (D, broken outlines) accumulate prematurely at the middle of the fusome (arrows). (**E-H**) Forming follicles: (E) schematic; mitochondria in *milt^{92}* null mutants remain at the anterior of the oocyte (G, small broken outline) and fail to form a normal Balbiani body (yellow broken outline) as in wild type (F). In *milt^{EY01559}* mutants, excess mitochondria move into the oocyte (H) to form an abnormally large Balbiani body. (**I-L**) Stage 5 follicles: (I) schematic; in wild type (J), mitochondria are sparse and evenly distributed. Mitochondria remain tightly packed at the anterior of *milt^{92}* oocytes (K, arrow). In *milt^{EY01559}*, mitochondria fill the cytoplasm of the oocyte (L). (**M-P**) Stage 9 follicles: (M) schematic; the number of mitochondria in wild type (N), *milt^{92}* (O) and *milt^{EY01559}* (P) is similar. However, in *milt^{EY01559}*, mitochondria cluster at the anterior of the oocyte (P, arrow), where microtubule minus-ends focus (M). (B-D,F-H,J-L,N-P) ATP synthase, green; (B-D,F,H) 1B1, magenta; (J-L,N-P) phosphotyrosine, magenta; (G) β-galactosidase marks wild type cells (blue). Scale bars: 10 μm in A-L; 20 μm in M-P.

Table 1. Penetrance of the mitochondrial distribution phenotypes

Mitochondrial distribution phenotype	*milt*^{92} clones	*Dhc64C*$^{6\text{-}6/6\text{-}12}$	*milt*^{EY01559}	*milt*^{K06704} clones	*milt*^{K14514}	*Khc*^{27} clones
Premature aggregation in prefollicular cysts (see Fig. 1B-D, Fig. 4B,C)	0% (0/16)	0% (0/25)	80% (42/53)	90% (9/10)	0% (0/9)	100% (35/35)
Abnormal Balbiani body size in forming follicles (see Fig. 1F-H, Fig. 4E,F)	Smaller 100% (13/13)	Smaller 85% (22/26)	Larger 100% (23/23)	Larger 100% (6/6)	Larger 0% (0/7)	Larger 100% (6/6)
Abnormal mitochondrial number in stage 2-5 follicles (see Fig. 1J-L)	Too few 100% (18/18)	Too few 92% (23/25)	Excess 100% (24/24)	Excess 100% (8/8)	Excess 100% (21/21)	Excess 100% (20/20)

Mitochondrial DNA

Genomic DNA was extracted from 120 stage 14 eggs dissected from wild-type and *milt*^{EY01559} ovaries. The DNA was digested with *Eco*R1 and run on an agarose gel to visually compare ethidium bromide stained bands.

RESULTS

Analysis of null *milt*^{92} germline clones showed that *milton* plays a role in Balbiani body formation (Table 1). Mitochondria in the mutant germ cells associated normally with the fusome in prefollicular cysts (Fig. 1B,C). However, when follicles formed, no evidence of mitochondrial transport into the oocyte was observed, and only about one-third of the normal number of mitochondria accumulated at the oocyte anterior (Fig. 1G). These probably represent the endogenous mitochondria of the oocyte, but in the absence of mitochondria from other germ cells their organization resembles their normal association with the fusome in younger cysts (Fig. 1B), rather than a Balbiani body. In older follicles (stage 5), when mitochondria normally disperse throughout much of the oocyte cytoplasm (Fig. 1I,J), *milt*^{92} mutant oocytes contained fewer mitochondria, which remained at the anterior (Fig. 1K, arrow). By stage 9, however, after the microtubule polarity in the oocyte has reorganized (Fig. 1M), mitochondria in *milt*^{92} germline clone oocytes had spread throughout the cytoplasm and reached approximately wild type numbers (compare Fig. 1N with 1O). This recovery appeared to provide adequate mitochondrial function to the oocyte. Zygotes lacking both maternal and zygotic *milt* function can complete embryogenesis and form a normal number of pole cells (see Fig. S2 in the supplementary material), but they die as second instar larvae (Stowers et al., 2002) (data not shown). These observations reveal that *milt* is required for normal Balbiani body formation, and suggest that a compensatory mechanism, such as over-replication, corrects the initial deficit in mitochondrial number.

Surprisingly, three different *milton* alleles (*milt*^{k14514}, *milt*^{EY01559} and *milt*^{k06704} – 'class II alleles') gave the opposite phenotype (Table 1). In class II mutants, mitochondria aggregated prematurely near and within the oocyte in prefollicular cysts (Fig. 1D, arrows). Mitochondria in *milt* class II mutants produced a giant Balbiani body that completely filled the cytoplasm of the oocyte at follicle formation (Fig. 1H). Mitochondrial number remained elevated at stage 5 (Fig. 1L), but by stage 9 it had normalized (Fig. 1P), again showing the existence of a compensatory mechanism. However, mitochondria still concentrated abnormally at microtubule minus ends in the anterior corners of these follicles (Fig. 1P, arrow). Nonetheless, females bearing class II alleles laid eggs with normal mtDNA content (see Fig. S2 in the supplementary material) that could be fertilized, form pole cells normally (see Fig. S2 in the supplementary material) and give rise to viable, fertile adults.

The failure of mitochondria to form a normal Balbiani body in *milt* mutants was not simply due to a general disruption of the fusome or of microtubule-dependent transport. The fusomes of *milt* cysts were indistinguishable from wild type throughout oogenesis (Fig. 2A-C). Organelles normally associated with the Balbiani body, such as Golgi elements, moved en masse into the oocyte at follicle formation on schedule (Fig. 2D-F). Cup protein, a marker for germ plasm components that are associated with the Balbiani body (Cox and Spradling, 2003; Wilhelm et al., 2003), was unaffected by *milt*

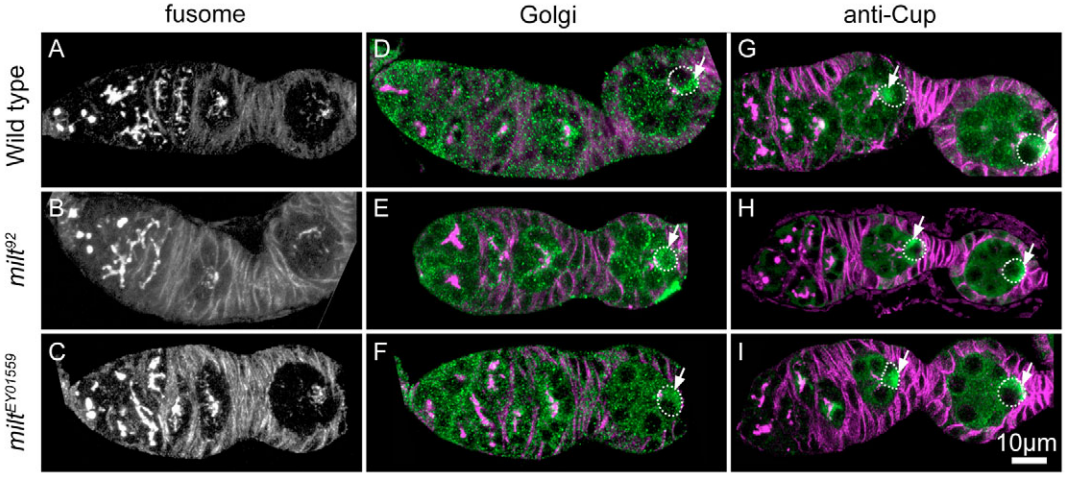

Fig. 2. Balbiani body-associated components are normal in *milt* mutants. (**A-C**) The fusome in *milt*^{92} null (B) and *milt*^{EY01559} class II mutants (C) is indistinguishable from wild type (A). (**D-F**) Golgi elements (green) concentrate and move into the oocyte (broken outline) normally; compare wild type (D, arrow) with *milt*^{92} (E, arrow) and *milt*^{EY01559} (F, arrow). (**G-I**) Cup protein (green) accumulates preferentially in the oocyte at the time of follicle formation in wild type (G, arrows) as well as in *milt*^{92} (H, arrows) and *milt*^{EY01559} (I, arrows). (A-C) 1B1; (D-F) mannosidase II, green; (G-I) Cup, green; (D-I) 1B1, magenta. Scale bar: 10 μm.

mutations. Cup was enriched near the oocyte in prefollicular cysts, and at the oocyte posterior shortly after follicle formation (Fig. 2G-I). These observations further support the view that Milton is a mitochondria-specific motor adaptor.

Molecular analysis of the *milt* alleles suggested a mechanism for these opposite effects on mitochondrial movement. Two major *milt* transcripts, *milt*-RA and *milt*-RB (Fig. 3A), encode protein isoforms that differ only at their N termini, which encode part of a Huntington Associated Protein (HAP-1) domain (Fig. 3B) (see Drysdale et al., 2005; Brickley et al., 2005). The $milt^{92}$ null allele is caused by a 2 bp deletion that creates an early frameshift in the coding region of both Milt isoforms and abolishes detectable Milt protein (Stowers et al., 2002). The class II alleles are all caused by *P* element insertions in the first intron of the *milt*-RA transcription unit (Fig. 3A). $milt^{k06704}$ is lethal, $milt^{k14514}$ adults occasionally survive, and $milt^{EY01559}$ is viable and fertile. In $milt^{EY01559}$ ovaries, RT-PCR analysis showed

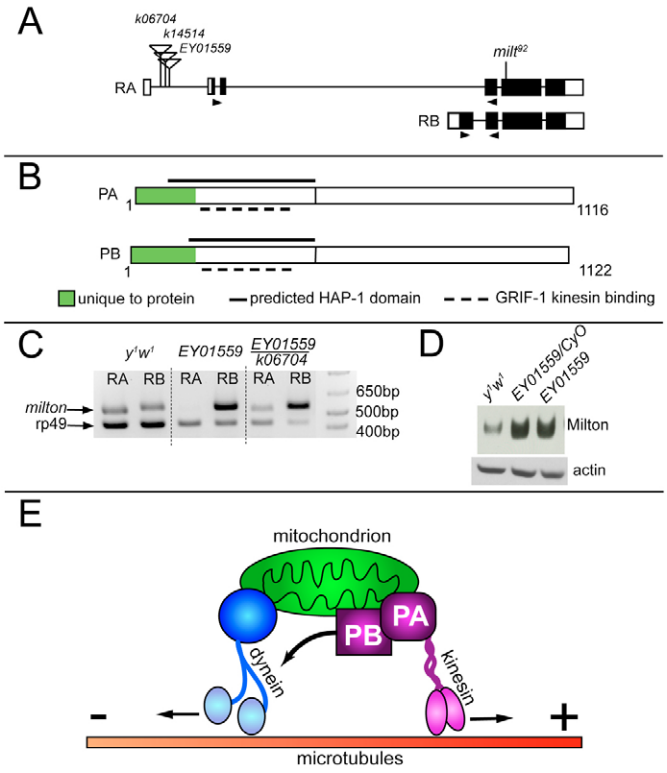

Fig. 3. *milt* mutants differentially express *milt* isoforms. (**A**) *milt* encodes two known transcripts, RA and RB. $milt^{92}$ contains a 2 bp deletion affecting both isoforms. The three class II alleles, *k06704*, *k14514* and *EY01559*, are all inserted within 100 bp of each other in the first intron of RA. Arrowheads indicate RT-PCR isoform-specific primer sites. (**B**) Two protein isoforms, Milt PA and PB, differ only at their N termini. Both contain the putative Kinesin-binding site, as uncovered for the mammalian homolog GRIF-1 using yeast two-hybrid analysis. However, some of their predicted HAP-1 domains differ. (**C**) RT-PCR shows that *milt* RA and RB are expressed equally in wild type. In $milt^{EY01559}$, RA is absent and RB is increased. In $milt^{EY01559/k06704}$, the ratio of RB to RA is still greatly elevated. (**D**) A Western blot shows that Milt is overexpressed in $milt^{EY01559}$ and $milt^{EY01559}$/*CyO* ovaries. The Milton antibody used recognizes both PA and PB. (**E**) Model of Milton-mediated bidirectional mitochondrial movement along microtubules. Milt-PA (magenta oval) and possibly Milt-PB (magenta square) link mitochondria to microtubules via the plus-end directed motor Kinesin. Additionally, Milt-PB positively influences the minus-end directed motor Dynein (large arrow).

that the level of the RA transcript is greatly reduced compared with wild type, while unexpectedly, the level of the RB transcript is substantially elevated (Fig. 3C). The relative amount of RB compared with RA transcript was also increased in viable, heteroallelic combinations of the other alleles (Fig. 3C). The increase in RB transcript levels overcompensates for the reduction in RA transcript levels, because mutant ovaries produce higher overall levels of Milt protein compared with wild type (Fig. 3D). A dominant effect on mitochondrial behavior during oogenesis was not observed (data not shown), possibly because in heterozygotes the ratio of the RA and RB isoforms is closer to normal.

These experiments suggest a simple model for Milt action (Fig. 3E). The Milt-PA isoform may mediate mitochondrial movement towards plus ends via Kinesin, while the Milt-PB form may exert a positive influence on minus-end directed movement via Dynein. This would explain why removing both isoforms blocks mitochondrial movement, whereas preferentially increasing the RB form favors minus-end directed movement. Therefore, we tested the model's predictions: (1) reducing Kinesin function should enhance mitochondrial movement into the oocyte, like *milt* class II alleles; and (2) reducing Dynein function should exert the opposite effect. Cysts completely lacking Kinesin heavy chain (Table 1) showed the same premature mitochondrial movement (Fig. 4B, arrow) and giant Balbiani body production (Fig. 4E, broken yellow line) as did cysts bearing class II *milton* alleles (Fig. 1D,H). These phenotypes in the Khc^{27} null clones equaled or surpassed the strongest class II *milton* mutant, $milt^{k06704}$. These phenotypes were also seen in older follicles (see Fig. S3 in the supplementary material). Thus, Milt-PA and Kinesin contribute to a 'reverse' force whose activity relative to minus-end directed forces controls the timing and extent of mitochondrial movement along microtubules into the oocytes of new follicles.

Testing the role of Dynein is complicated by its known requirement to form normal 16-cell cysts (McGrail and Hays, 1997), and specify the oocyte (reviewed by Huynh and St Johnston, 2004). We examined female sterile adults bearing a viable combination of Dynein heavy chain alleles, $Dhc64C^{6-6/6-12}$ (Table 1) and found that their mitochondrial organization appears normal in prefollicular cysts (Fig. 4C). At the time of follicle formation, however, few if any mitochondria entered the oocyte, and only a very small Balbiani body was produced, presumably from the endogenous mitochondria of the oocyte (Fig. 4F). Although in projection this difference appears very small, analysis in three dimensions reveals a very substantial reduction in mitochondrial number (Fig. S4), as in $milt^{92}$ null clones. Only the fact that Cup protein still accumulated in a single posterior cell in most cysts allowed us to identify the oocyte, and indicated that oocyte specification had not simply been blocked (Fig. 4F, inset). Thus, reducing *Dhc* function has the opposite effect on mitochondrial behavior, as reducing *Khc* function, supporting the prediction that Milt stimulates minus end movement via Dynein, in addition to acting via Kinesin.

Dhc molecules normally become enriched in the oocyte cytoplasm beginning in prefollicular cysts (Fig. 4G,H) (Li et al., 1994). It is not known what fraction of these motors are engaged in mitochondrial transport in ferrying other components, or lack cargos entirely. Despite the dramatic changes in mitochondrial transport in $milt^{EY01559}$ follicles, the timing and level of Dhc accumulation was unaffected (Fig. 4I,J). Similar results were observed for $milt^{92}$ null clones (data not shown). This suggests that mitochondrial movement in wild type is not tightly linked to Dynein levels, but controlled by the amount or state of the Milton adaptors.

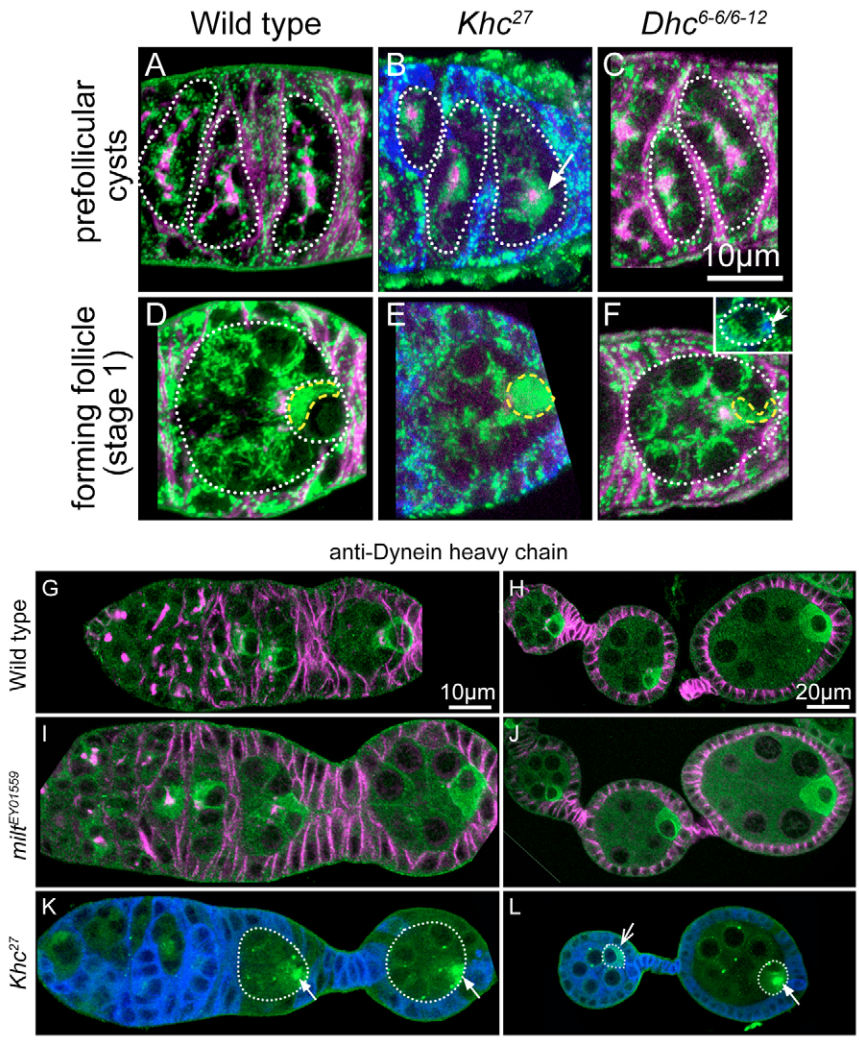

Fig. 4. *Khc* mutants resemble *milt* class II mutants. (**A-C**) Prefollicular cysts: mutant *Khc*^{27} clonal cysts (B, broken outlines) show premature mitochondrial accumulation (green, arrow) at the middle of the fusome (magenta) in contrast to wild-type (A) and *Dhc64C*$^{6\text{-}6/6\text{-}12}$ (C) cysts. (**D-F**) Forming follicles: the Balbiani body (broken yellow line) is greatly enlarged in *Khc*^{27} clones (E) and reduced in *Dhc64C*$^{6\text{-}6/6\text{-}12}$ mutants (F) compared with wild type (D). The *Dhc64C*$^{6\text{-}6/6\text{-}12}$ oocyte (F inset, barbed arrow) can be distinguished from the nurse cells by its selective accumulation of Cup protein (blue). (**G-J**) Dynein heavy chain (green) localization is indistinguishable between wild type (G,H) and *milt*^{EY01559} (I,J), both during follicle formation (G,I) and in older follicles (H,J). By contrast, Dhc accumulates in intense puncta in the posterior region of *Khc*^{27} mutant oocytes (arrows, **K**,**L**). A wild-type oocyte shows normal diffuse Dhc localization (L, barbed arrow). (A-F) ATP synthase, green; (G-L) Dynein heavy chain, green; (A-J) 1B1, magenta; (B,E,K,L) β-galactosidase marks wild-type cells (blue). Scale bars: 10 μm in A-F; 10 μm in G,I,K; 20 μm in H,J,L.

Centrioles, specific RNAs, Golgi and probably other cargos in addition to mitochondria are transported into the oocyte at the time of follicle formation (Cox and Spradling, 2003). Their movement may also use plus and minus-end directed motors controlled by different adaptor molecules. Removing the Khc motor should accelerate the movement into the oocyte of all cargos on which Kinesin opposes the action of Dynein. We observed that oocytes bearing *Khc*^{27}-null clones accumulate excess amounts of Dhc (compare Fig. 4K,L with 4G,H). In addition, Dhc molecules in the mutant clones appear aggregated and concentrated towards the oocyte posterior, the locus of microtubule minus ends. This suggests that most cargos transported into the early oocyte are controlled, like mitochondria, by the opposing activity of Khc and Dhc motors.

Further studies showed that *milt* is required for normal mitochondrial behavior in several different types of ovarian cells. The follicular epithelium is polarized, with microtubule minus ends oriented towards the apical surface (Clark et al., 1997) (Fig. 5A). In young follicles, mitochondria are normally found throughout the cytoplasm of the follicle cells (Fig. 5B, arrow) and loss of *milt* function (in *milt*^{92} follicle cell clones) did not alter their distribution (Fig. 5C, broken outline). However, follicle cell mitochondria dramatically clump at the apical surfaces of young follicle cells containing the strongest *milt* class II allele, *milt*^{k06704} (*n*=18/18, Fig. 5D, arrow). Later in follicle development, other systems of mitochondrial localization must come into play, because class II mutations did not affect mitochondrial distribution in follicles older than stage 7 (not shown). Mitochondrial aggregation at microtubule minus ends in follicle cells could be mimicked by disrupting Kinesin heavy chain, as in the case of forming oocytes (*n*=17/17, Fig. 5E, arrow), but again only up to stage 7 (Fig. 5E, asterisk). Thus, a Milton and Khc-dependent process disperses mitochondria during some but not all stages of developing ovarian follicles.

Similar studies of the mitochondrial distribution in germ line stem cells (GSCs) revealed unexpected new information about their microtubule organization. Mitochondria normally cluster on the apical side of GSCs (Fig. 5F, arrows) around the spectrosome, the fusome precursor located near their junction with cap cells. This localization was unaffected in *milt*^{92} null clones (Fig. 5G, arrow). However, in *milt*^{k06704} (*n*=8/8, Fig. 5H, arrow) and *Khc*^{27} (*n*=17/25, Fig. 5I, arrow) mutant germline stem cells, all the mitochondria clumped at the opposite side away from the spectrosome. Mitochondria are normally dispersed in forming cysts (Fig. 5L), but similar aggregations were frequently seen opposite the fusome when such cysts lacked Khc (*n*=42/60, Fig. 5I,M). Because one spindle pole is always found near the spectrosome during stem cell mitosis and because centrioles have been localized there in electron micrographs (Lin et al., 1994), it had been assumed that microtubule minus ends cluster apically throughout the cell cycle. Our observations indicate that microtubules in stem cells and forming

cysts are dynamic (Grieder et al., 2000), and that a significant fraction of microtubules in these cells have a different orientation during interphase (Fig. 5J,K) than at mitosis.

DISCUSSION

The Balbiani body, a large aggregate of mitochondria frequently associated with other membranous organelles and germ plasm components, is found in the newly formed oocytes of diverse species. Although it has been postulated to play a role in germ cell development and mitochondrial inheritance, no function for the Balbiani body has been demonstrated (reviewed by Kloc et al., 2004). Previously, we have identified the *Drosophila* Balbiani body and showed that it arises when a large number of mitochondria from sister germ cells associate with the fusome, move towards its center and enter the oocyte en masse where they supplement the pre-existing mitochondria of the oocyte (Cox and Spradling, 2003). Like ooctye development itself, Balbiani body formation requires the genes *hts* and *egl*, suggesting that mitochondrial movement depends on Dynein/dynactin-mediated minus-end directed transport along polarized microtubules (Cox and Spradling, 2003) (reviewed by Huynh and St Johnston, 2004). Our studies of the mitochondrial adaptor protein Milton and its partner Kinesin heavy chain (Glater et al., 2006) now show that plus-end directed mitochondrial transport determines when and how large a Balbiani body will form. We have also carried out the first test of Balbiani body function.

Mitochondrial position within cells of diverse types is frequently regulated by motor-dependent transport along microtubules (reviewed by Welte, 2004; Gross, 2004). Often such positioning optimizes the ability of mitochondria to generate energy or metabolic products in appropriate subcellular locations (reviewed by Hollenbeck and Saxton, 2005). In *Drosophila* photoreceptors, neurons and in cultured cells, Milton plays a key role in positioning mitochondria by acting as a adaptor molecule between mitochondria and the Khc plus-end-directed microtubule motor (Stowers et al., 2002; Glater et al., 2006). We found that null *Khc* mutations and type II *milt* alleles cause premature entry of an excess number of mitochondria into the oocyte. This suggests that the orchestrated movement of mitochondria within germline cysts and its sudden entry into the oocyte during follicle formation is controlled by plus-end directed transport machinery that opposes Dynein-mediated minus-end directed movement towards the oocyte. Plus-end directed activity is not needed for mitochondria to associate with the fusome, as normal fusome interactions were still observed in the absence of *Khc* or *milt* function. However, the opposing action of Milt and Khc appeared to be particularly effective near ring canals, especially the four oocyte ring canals, just outside of which mitochondria accumulate for a period of 1-2 days prior to follicle formation. As a new follicle prepares to bud off, an unknown modulation relieves the standoff and leads to the rapid influx of mitochondria into the oocyte where they coalesce with endogenous mitochondria to form the Balbiani body. In the absence of any movement, as in $milt^{92}$ cysts, or in cysts with compromised Dhc function, a much smaller cluster of mitochondria forms in the oocyte, made up only of organelles inherited during germ cell divisions.

Complete loss of Milton did not enhance mitochondrial movement into the oocyte, as expected if its sole function was linkage to Khc. Instead, we found that *milt* is needed for both minus-end directed and plus-end directed movement. Upregulation of Milt-PB relative to Milt-PA favors Dynein-based movement, but the basis for this effect remains unclear. Both Milt isoforms contain a common Kinesin binding domain, and associate with Kinesin in vivo (Stowers et al., 2002; Glater et al., 2006). Evidence that Milt proteins bind Dynein directly is lacking, and the related GRIF1 protein does not bind Dynein (Brickley et al., 2005). Thus, Milt-PB probably promotes linkage of mitochondria to Dynein indirectly, perhaps by binding and modulating Dynactin. Consistent with this view, the HAP-1 domain that differs between the two isoforms has been predicted to mediate interaction with Dynactin (Li et al., 1998).

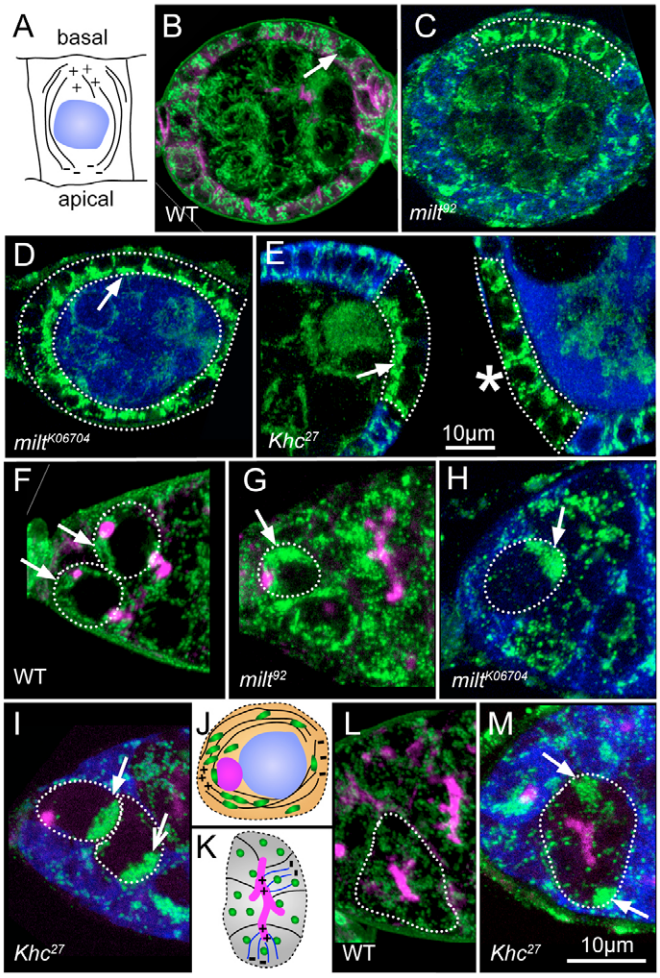

Fig. 5. Mitochondrial mislocalization in *milt* class II mutants reveals microtubule polarity. (**A**) Known apical polarity of microtubules in follicular epithelial cells. (**B**,**C**) Mitochondria (green) are evenly distributed in wild type (B, arrow) and $milt^{92}$ mutant (C, broken outline) follicle cells. (**D**,**E**) Mitochondria cluster at the apical side of $milt^{k06704}$ mutant follicle cells (D, arrow), as predicted (A). Khc^{27} mutant follicle cells also accumulate mitochondria at their apical surface (E, arrow) until stage 7, when mitochondrial distribution becomes normal (E, asterisk). (**F**,**G**) Mitochondria predominantly localize at the anterior end of wild-type (F, arrows) and $milt^{92}$ mutant (G, arrow) GSCs (broken outlines) near the spectrosome (magenta). By contrast, in $milt^{k06704}$ mutant clones (**H**, arrow) and Khc^{27} mutant clones (**I**, arrow) mitochondria aggregate at the posterior of the GSC (broken outlines). This suggests the minus ends of the microtubules are directed towards the posterior of the stem cell, away from the spectrosome (**J**). (**K-M**) Mitochondria in dividing cysts are normally spread evenly throughout the cytoplasm (L, broken outline). However, they clump away from the fusome (magenta) in $Khc^{2\ 7}$ clones (I, barbed arrow; M, arrows), indicating the location of microtubule minus ends (K). (B-I,L,M) ATP synthase, green; (B,F,G,I,L,M) 1B1, magenta; (C-E,H,I,M) β-galactosidase marks wild-type cells (blue). Scale bars: 10 μm in B-E; 10 μm in F-M.

Thus, changes in the relative amounts of Milt isoforms, and in their interactions with mitochondria appear to regulate the location of these organelles.

Related mechanisms may control the movement along the fusome and entry into the oocyte of other cargos besides mitochondria. Organelles such as Golgi elements, and specific mRNAs such as *Bic-D*, *oskar* and *cup* localize towards the center of developing 16-cell cysts, and enter the oocyte (Cox and Spradlling, 2003) (reviewed by Huynh and St Johnston, 2004). *oskar* and *cup* RNA transiently associate with the Balbiani body in forming follicles (Cox and Spradling, 2003). However, all these RNAs localize to the initial cyst cell earlier than mitochondria (Cox and Spradling, 2003), and we found that Cup continues to accumulate preferentially in the oocyte even in $Dhc64C^{6\text{-}6/6\text{-}12}$ mutants that block mitochondrial transport. Consequently, even if all these components are localized based an interplay of plus-end- and minus-end-directed micotubule transport, their movement towards the oocyte is regulated differently, possibly because each is linked by cargo-specific adaptors.

Finally, these experiments provide the first test of Balbiani body function. The initial wave of mitochondria that enter the oocyte of new follicles in the Balbiani body have been proposed to have high fitness, and to represent the inheritance bottleneck of mitochondrial genomes (Pepling and Spradling, 2001; Cox and Spradling, 2003). We find that oocytes from *milt* alleles, where this process has been strongly disrupted, still give rise to viable and fertile offspring. In part, this may be due to our observation that an independent system of mitochondrial copy number control acts to correct initial increases or deficits in oocyte mitochondrial number. Future studies will be required to determine if mitochondrial inheritance patterns are altered in *milt* class II mutants, and if the offspring of these alleles suffer an increased incidence of mitochondrial dysfunction over their lifespan.

We thank Dr Tom Schwarz for providing several of the *milt* alleles and for anti-Milt antibody, and Dr Rafael Garasse for the anti-ATP-synthase antibody.

Supplementary material

Supplementary material for this article is available at
http://dev.biologists.org/cgi/content/full/133/17/3371/DC1

References

Bellen, H. J., Levis, R. W., Liao, G., He, Y., Carlson, J. E., Tsang, G., Evans-Holm, M., Hiesinger, R., Schulze, K. L., Rubin, G. M. et al. (2004). The BDGP gene disruption project: single transposon insertions associated with 40% of Drosophila genes. *Genetics* **167**, 761-781.

Bolivar, J., Huynh, J. R., Lopez-Schier, H., González, C., St Johnston, D. and González-Reyes, A. (2001). Centrosome migration into the Drosophila oocyte is independent of BicD, egl and of the organisation of the microtubule cytoskeleton. *Development* **128**, 1889-1897.

Brickley, K., Smith, M. J., Beck, M. and Stephenson, F. A. (2005). GRIF-1 and OIP106, members of a novel gene family of coiled-coil domain proteins: association in vivo and in vitro with kinesin. *J. Biol. Chem.* **280**, 14723-14732.

Clark, I. E., Jan, L. Y. and Jan, Y. N. (1997). Reciprocal localization of Nod and kinesin fusion proteins indicates microtubule polarity in the Drosophila oocyte, epithelium, neuron and muscle. *Development* **124**, 461-470.

Cox, R. T. and Spradling, A. C. (2003). A Balbiani body and the fusome mediate mitochondrial inheritance during Drosophila oogenesis. *Development* **130**, 1579-1590.

de Cuevas, M. and Spradling, A. C. (1998). Morphogenesis of the Drosophila fusome and its implications for oocyte specification. *Development* **125**, 2781-2789.

Drysdale, R. A., Crosby, M. A. and The FlyBase Consortium (2005). FlyBase: genes and gene models. *Nucleic Acids Res.* **33**, D390-D395.

Glater, E. E., Megeath, L. J., Stowers, R. S. and Schwarz, T. L. (2006). Axonal transport of mitochondria requires Milton to recruit kinesin heavy chain and is light chain independent. *J. Cell Biol.* **173**, 545-557.

Gorska-Andrzejak, J., Stowers, R. S., Borycz, J., Kostyleva, R., Schwarz, T. L. and Meinertzhagen, I. A. (2003). Mitochondria are redistributed in Drosophila photoreceptors lacking Milton, a kinesinassociated protein. *J. Comp. Neurol.* **463**, 372-388.

Grieder, N. C., de Cuevas, M. and Spradling, A. C. (2000). The fusome organizes the microtubule network during oocyte differentiation in Drosophila. *Development* **127**, 4253-4264.

Gross, S. P. (2004). Hither and yon: a review of bi-directional microtubule-based transport. *Phys. Biol.* **1**, R1-R11.

Guraya, S. S. (1979). Recent advances in the morphology, cytochemistry and function of Balbiani's vitelline body in animal oocytes. *Int. Rev. Cytol.* **59**, 249-321.

Hollenbeck, P. J. and Saxton, W. M. (2005). The axonal transport of mitochondria. *J. Cell Sci.* **118**, 5411-5419.

Huynh, J. R. and St Johnston, D. (2004). The origin of asymmetry: early polarisation of the Drosophila germline cyst and oocyte. *Curr. Biol.* **14**, R438-R449.

Huynh, J. R., Shulman, J. M., Benton, R. and St Johnston, D. (2001). PAR-1 is required for the maintenance of oocyte fate in Drosophila. *Development* **128**, 1201-1209.

Keyes, L. and Spradling, A. C. (1997). The Drosophila gene *fs(2)cup* interacts with *otu* to define a cytoplasmic pathway required for the structure and function of germline chromosomes. *Development* **124**, 1419-1431.

Kloc, M., Bilinski, S. and Etkin, L. D. (2004). The Balbiani body and germ cell determinants: 150 years later. *Curr. Top. Dev. Biol.* **59**, 1-36.

Li, M., McGrail, M., Serr, M. and Hays, T. S. (1994). Drosophila cytoplasmic dynein, a microtubule motor that is asymmetrically localized in the oocyte. *J. Cell Biol.* **126**, 1475-1494.

Li, S.-H., Gutekunst, C.-A., Hersch, S. M. and Li, X.-J. (1998). Interaction of Huntingtin-associated protein with dynactin p150Glued. *J. Neurosci.* **18**, 1261-1269.

Lin, H., Yue, L. and Spradling, A. C. (1994). The Drosophila fusome, a germline-specific organelle, contains membrane skeleton proteins and functions in cyst formation. *Development* **120**, 947-956.

Mahowald, A. P. and Strassheim, J. M. (1970). Intercellular migration of centrioles in the germarium of Drosophila melanogaster. An electron microscopic study. *J. Cell Biol.* **45**, 306-320.

Matova, N. and Cooley, L. (2001). Comparative aspects of animal oogenesis. *Dev. Biol.* **231**, 291-320.

McGrail, M. and Hays, T. S. (1997). The microtubule motor cytoplasmic dynein is required for spindle orientation during germline cell divisions and oocyte differentiation in Drosophila. *Development* **124**, 2409-2419.

Moreman, K. W., Touster, O. and Robbins, P. W. (1991). Novel purification of the catalytic domain of Golgi alpha-mannosidase II. Characterization and comparison with the intact enzyme. *J. Biol. Chem.* **266**, 16876-16885.

Pepling, M. E. and Spradling, A. C. (2001). Mouse ovarian germ cell cysts undergo programmed breakdown to form primordial follicles. *Dev. Biol.* **234**, 339-351.

Serbus, L. R., Cha, B. J., Theurkauf, W. E. and Saxton, W. M. (2005). Dynein and the actin cytoskeleton control kinesin-driven cytoplasmic streaming in Drosophila oocytes. *Development* **132**, 3743-3752.

Stowers, R. S., Megeath, L. J., Gorska-Andrzejak, J., Meinertzhagen, I. A. and Schwarz, T. L. (2002). Axonal transport of mitochondria to synapses depends on Milton, a novel Drosophila protein. *Neuron* **36**, 1063-1077.

Theurkauf, W., Alberts, B., Jan, Y. and Jongens, T. (1993). A central role for microtubules in the differentiation of Drosophila oocytes. *Development* **118**, 1169-1180.

Welte, M. A. (2004). Bidirectional transport along microtubules. *Curr. Biol.* **14**, R525-R537.

Wilhelm, J. E., Mansfield, J., Hom-Booher, N., Wang, S., Turck, C. W., Hazelrigg, T. and Vale, R. D. (2000). Isolation of a ribonucleoprotein complex involved in mRNA localization in Drosophila oocytes. *J. Cell Biol.* **148**, 427-440.

Wilhelm, J. E., Hilton, M., Amos, Q. and Henzel, W. J. (2003). Cup is an eIF4E binding protein required for both the translational repression of oskar and the recruitment of Barentsz. *J. Cell Biol.* **163**, 1197-1204.

Supplementary Figure 1.

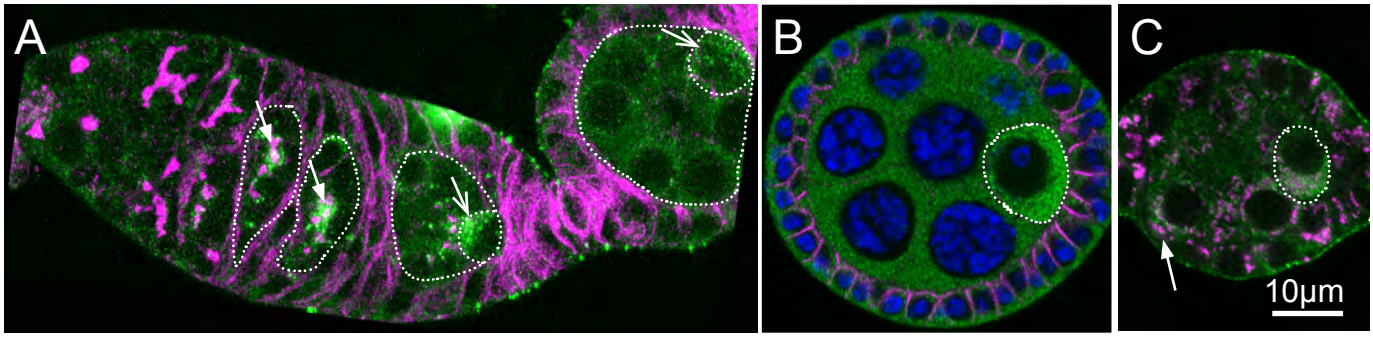

Milton localization in the ovary. (A) Milton (green) accumulates around the fusome (magenta) in pre-follicular cysts (dashed outlines, arrows). As the follicle forms and buds, Milton accumulates in the oocyte (barbed arrows, small dashed outlines). Milton is also found in punctae throughout the germ cell cytoplasm. (B) Milton continues to concentrate in the oocyte (dashed outline) and is also found diffusely in the cytoplasm of other cyst cells. (C) Milton co-localizes with mitochondria (magenta) in general (arrow), including the Balbiani body in forming follicles (barbed arrow, dashed outline). (A-C) green = Milt (A, B) magenta = 1B1 (C) magenta = ATPsynthase (B) blue = DAPI.

Supplementary Figure 2

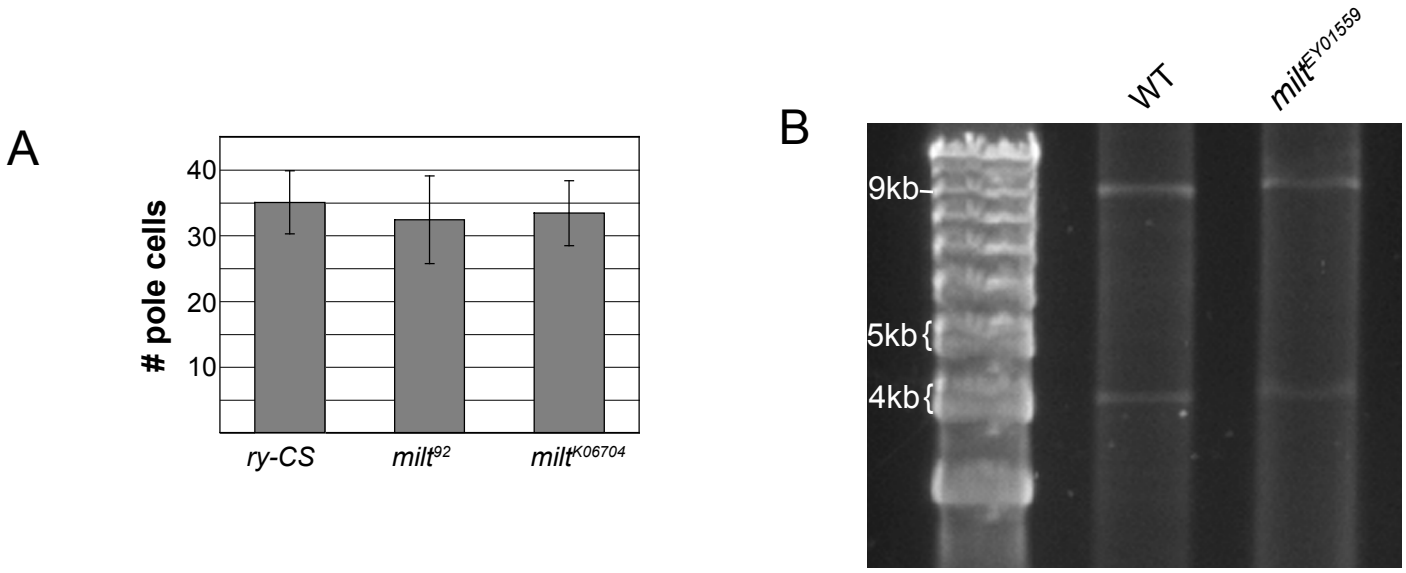

Pole cell formation and mtDNA content is normal in *milt* mutants. (A) The normal number of pole cells form in maternally mutant *milt* embryos for both $milt^{92}$ null and $milt^{K06704}$ class II mutants. (B) The amount of mitochondrial DNA in stage 14 eggs is approximately the same between wild type and $milt^{EY01559}$.

Supplementary Figure 3

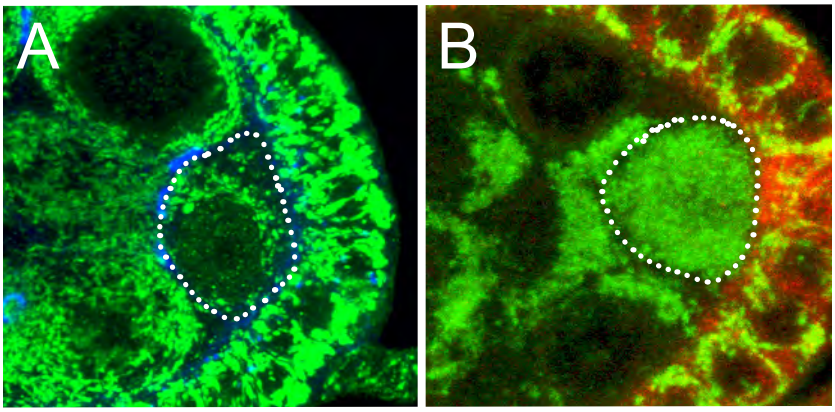

Older follicles (stage 5) homozygous for *Khc*^{27} (B) contain excessive mitochondria in their oocytes (white dashed line) compared to corresponding wild type follicles (A). green = ATP synthase (mitochondria); blue = phosphotyrosine (ring canals); red = beta-galactosidase.